Response of Simulated Squall Lines to Low-Level Cooling

MATTHEW D. PARKER

Department of Marine, Earth, and Atmospheric Sciences, North Carolina State University, Raleigh, North Carolina

(Manuscript received 1 May 2007, in final form 31 July 2007)

ABSTRACT

Organized convection has long been recognized to have a nocturnal maximum over the central United States. The present study uses idealized numerical simulations to investigate the mechanisms for the maintenance, propagation, and evolution of nocturnal-like convective systems. As a litmus test for the basic governing dynamics, the experiments use horizontally homogeneous initial conditions (i.e., they include neither fronts nor low-level jet streams).

The simulated storms are allowed to mature as surface-based convective systems before the boundary layer is cooled. In this case it is then surprisingly difficult to cut the mature convective systems off from their source of near-surface inflow parcels. Even when 10 K of the low-level cooling has been applied, the preexisting system cold pool is sufficient to lift boundary layer parcels to their levels of free convection. The present results suggest that many of the nocturnal convective systems that were previously thought to be elevated may actually be surface based. With additional cooling, the simulated systems do, indeed, become elevated. First, the CAPE of the near-surface air goes to zero: second, as the cold pool's temperature deficit vanishes, the lifting mechanism evolves toward a bore atop the nocturnal inversion. Provided that air above the inversion has CAPE, the system then survives and begins to move at the characteristic speed of the bore. Interestingly, as the preconvective environment is cooled and approaches the temperature of the convective outflow, but before the system becomes elevated, yet another distinct behavior emerges. The comparatively weaker cold pool entails slower system motion but also more intense lifting, apparently because it is more nearly balanced by the lower-tropospheric shear. This could explain the frequent observation of intensifying convective systems in the evening hours without the need for a nocturnal low-level jet. The governing dynamics of the simulated systems, as well as the behavior of low-level tracers and parcel trajectories, are addressed for a variety of environments and degrees of stabilization.

1. Introduction

Thunderstorms and mesoscale convective systems (MCSs) have long been recognized to have a nocturnal maximum over the central United States (e.g., Wallace 1975; Maddox 1980). As well, MCSs commonly occur on the cold side of midlatitude warm and stationary fronts [e.g., the "type-1 events" reviewed by Fritsch and Forbes (2001)]. It has frequently been assumed that convection is "elevated" when it occurs at night or on the cold side of a front, and Colman (1990) claimed that most cold season thunderstorms (outside of Florida) were likely of the elevated type.

For the purposes of this paper, a convective system is said to be *elevated* if it is not ingesting air from the near-surface layer (e.g., the lowest 500 m or so). Other colloquial definitions for elevated convection abound, but this one is physically robust and closely follows the definition in the *Glossary of Meteorology* (Glickman 2000). Conversely, a system that *is* ingesting air from the lowest levels is here called *surface based*, regardless of whether that air has the greatest potential buoyancy (i.e., the "most unstable" CAPE) in the sounding or not. The present study focused on the conditions in which long-lived convective systems may be elevated versus surface based, and the dynamics distinguishing and governing the two phases.

Elevated MCSs are thought to be decoupled from the stable planetary boundary layer air that lies beneath them. Previous authors have commented on the likelihood that the stable nocturnal or postfrontal boundary layer would inhibit deep penetrative downdrafts from aloft (e.g., Trier and Parsons 1993), and would create a

Corresponding author address: Dr. Matthew Parker, Campus Box 8208, North Carolina State University, Raleigh, NC 27695-8208.
E-mail: mdparker@ncsu.edu

DOI: 10.1175/2007JAS2507.1

regime more favorable for the propagation of trapped internal gravity waves or bores (e.g., Carbone et al. 1990). In such cases, the classical propagation mechanism of lifting by a surface cold pool (e.g., Rotunno et al. 1988) does not seem to apply. Indeed, some examples (e.g., Maddox 1980; Trier and Parsons 1993) reveal that the passage of an elevated MCS may be marked by minimal changes in the surface temperature. Even so, at least a subset of MCSs are known to produce severe winds at night and on the cold side of fronts (e.g., Johns and Hirt 1987; Kuchera and Parker 2006). One possibility is that such systems are still cold pool driven and surface based, despite their comparatively stable boundary layers. For example, the simulations of Coniglio and Stensrud (2001), in a composite derecho environment, appear to exemplify this behavior.

Numerous case studies, extending back through those by Maddox (1983) and Wetzel et al. (1983), have documented the basic synoptic meteorological patterns and mesoscale flow regimes associated with nocturnal MCSs, including the frequent presence of a nocturnal temperature inversion, a low-level jet with significant attendant warm advection, and an elevated maximum in equivalent potential temperature (θ_e). Fritsch and Forbes (2001) dubbed such cases "type 1" convective systems, and noted that a synoptic front often is present to assist in lifting warm sector air parcels. Indeed, in their review they point out numerous examples in which lower-tropospheric warm advection and isentropic ascent are fundamental to the environments of MCSs.

There are a wide variety of case study simulations that have included elevated convection on the cool side of fronts [i.e., the type-1 systems of Fritsch and Forbes (2001)]. For example, Trier et al. (2006) provided a detailed study of the role of mesoscale features (fronts, low-level jets, etc.) in fashioning the environment for simulated elevated convective storms. However, as shown by Cotton et al. (1983) and Wetzel et al. (1983), nighttime convective systems over the central United States often develop as surface-based storms earlier in the day over the high terrain to the west. As a litmus test for the basic dynamics governing such convection, the present numerical experiments use horizontally homogeneous initial conditions (i.e., they include neither fronts nor low-level jet streams). A cold-pool-driven convective system develops in the base-state environment [i.e., the "type 2" systems of Fritsch and Forbes (2001)]; low-level cooling is then applied, mimicking the evolution of an MCS as the sun sets (or, as the MCS crosses a front). Subsequent convection could possibly be maintained by lifting air from above the stabilized layer; or, if the surface cold pool persists, convection could possibly be maintained by air from within the stabilized layer, provided that it has convective available potential energy (CAPE) and that the cold pool provides sufficient lifting to overcome any convective inhibition (CIN) that is present.

Within a typical statically stable environment, convectively generated mass and momentum perturbations lead to tropospheric gravity waves. For example, convective systems produce internal gravity waves with both high and low frequencies; Fovell et al. (2006) recently provided a nice review of both sorts of convectively generated waves, while analyzing their forms and impacts within the troposphere. In addition to these tropospheric internal waves, convective systems also produce low-level outflow as a result of convective cooling. The form taken by this outflow is an important element of the present experiments that include boundary layer cooling. For example, Raymond and Rotunno (1989) and Haertel et al. (2001) have shown that changes to the low-level stability impact whether an outflow is mainly in the form of a density current or gravity waves. In statically neutral conditions (i.e., the afternoon boundary layer), the lower-tropospheric response to cooling is a density current. Such density current outflows are often the mechanism for self-regenerating convective systems (e.g., Rotunno et al. 1988). However, the response of a statically stable boundary layer to cooling is at least partly in the form of gravity waves along the stable layer. Even though the simulations of Raymond and Rotunno (1989) and Haertel et al. (2001) did not include actual self-regenerating convective systems, a reasonable inference from their studies is that low-level gravity wave outflows could become the primary mechanism for convective redevelopment if the waves both (i) move into the environment more quickly than the density current response, and (ii) produce enough vertical displacement to lift low-level air to its level of free convection (LFC).

Schmidt and Cotton (1990) modeled an elevated convective system whose rapid speed they attributed to such wave propagation. In essence, the system's main updraft region was directly above the hump in the isentropes associated with the gravity wave. Buzzi et al. (1991) also simulated a squall line with a stable boundary layer and noted the presence of a "large amplitude solitary gravity wave" in the low levels. In these two studies, as well as in some of the simulations of Dudhia et al. (1987), boundary layer parcels underwent vertical excursions but then descended again without reaching their LFCs; the convective updrafts were fed from aloft and appeared to be decoupled from the low-level flow. Although the gravity waves did not raise near-surface

parcels to their LFCs, the hump in the isentropes associated with the wave provided lifting for air parcels *above* the stable layer. Schmidt and Cotton (1990) emphasized the phasing between upper- and lower-tropospheric gravity waves in shear and they also reviewed some other historical theories about the relationship of gravity waves to squall line propagation. In the present paper, low-level gravity wave outflows are treated somewhat simply as mechanisms for the lifting of lower-tropospheric air parcels to their LFCs, without reference to some of the more extravagant feedbacks that may occur thereafter.

When a well-developed density current encounters a stable layer, an internal bore can also result (e.g., Klemp et al. 1997). Carbone et al. (1990) discussed regeneration of nocturnal convection by an undular bore and noted that the bore response lay in the middle of a continuum between pure density current outflows (dominated by mass transport) and pure gravity wave outflows (having no mass transport). They noted evolution in time from the density current mode toward internal bores, and finally solitary gravity waves as energy was dissipated from the disturbance within the stable boundary layer. Recent high-resolution observations by Knupp (2006) showed a very similar progression. Liu and Moncrieff (2000) noted that these various outflow modes can coexist in environments with intermediate stratification, and simulated complex multiheaded density currents with "solitary wave-like or bore-like disturbances" propagating out ahead of the current. Haertel et al. (2001) also discussed scenarios in which convective outflow may be expressed in terms of combinations of the density current and gravity wave processes. In effect, bore dynamics can resemble those of either phenomenon. For example, Klemp et al. (1997) noted that, as the depth of the prebore stable layer decreases, the speed of the bore approaches the density current speed and, as depth of the prebore stable layer increases, the speed of the bore approaches the intrinsic gravity wave speed.

For such reasons, Haertel et al. (2001) eschewed the term "bore" (they found it to be ambiguous). In the present study, wavelike disturbances are accompanied by a "sudden, and relatively permanent change" in velocity and in the height of the stable layer's top [i.e., the definition of Locatelli et al. (1998)]. Fluid passes through the disturbances, rather than being lifted up and over them [i.e., as described and analyzed by Klemp et al. (1997)]. Thus, the disturbances will be referred to as bores, although they share some properties with solitary gravity waves.

Both Dudhia et al. (1987) and Buzzi et al. (1991) found that the lower-tropospheric shear was important to the sustenance of wave-driven convection in the presence of a lower-tropospheric stable layer. Furthermore, the vertical wind shear helped determine whether the gravity wave or density current mode of lifting predominated in the simulations of Dudhia et al. (1987). In the present simulations, the vertical wind shear was not varied among the experiments, but was simply set to an intermediate value (section 3) so that attention could be focused elsewhere.

The principal goal of this study is to understand the evolution of the convection as the boundary layer slowly becomes more stable with time. The novelty of the present simulations, when compared to those reviewed above, is in the slow introduction of the low-level cooling. As well, the present simulations are 3D, permitting a more realistic variety of convective storm types and trajectories than the preceding studies. Finally, the present simulations may be the first with sufficient vertical and horizontal resolution [on the order of that recommended by Bryan et al. (2003)] to depict the differing internal processes associated with surface-based versus elevated storms. These simulations are meant primarily to mimic the evolution of organized convection as the sun sets, a situation that is frequently realized in nature [e.g., the scenario of Cotton et al. (1983) and Wetzel et al. (1983)].

2. Method

This work incorporated 2D and 3D simulations using version 1.10 of the nonhydrostatic cloud model described by Bryan and Fritsch (2002). Because it was not possible to perform every simulation at high resolution in 3D, the 2D simulations were used to explore the parameter space for this study. The 2D sensitivity experiments, along with several 3D control runs, were then used to select a subset of 3D "production runs." The 2D and 3D simulations were very similar in terms of the convective structures and systems' evolutions; even so, the limitations of 2D simulations are well known. Therefore, all of the detailed analyses that follow are strictly from the 3D simulations.

To represent convective clouds, the simulations used ice microphysics [the Lin et al. (1983) scheme, with modifications as described by Braun and Tao (2000)]. All simulations had horizontal grid spacings of 250 m and a maximum vertical grid spacing of 250 m, which decreased progressively to 100 m below $z = 3500$ m. The condensed grid in the lower troposphere improved the depiction of "nocturnal" stable layers in the model. The 2D simulations used a grid that was 800×20 km; the 3D simulations used a grid that was $400 \times 60 \times 20$ km. In both cases, the along-line dimension was peri-

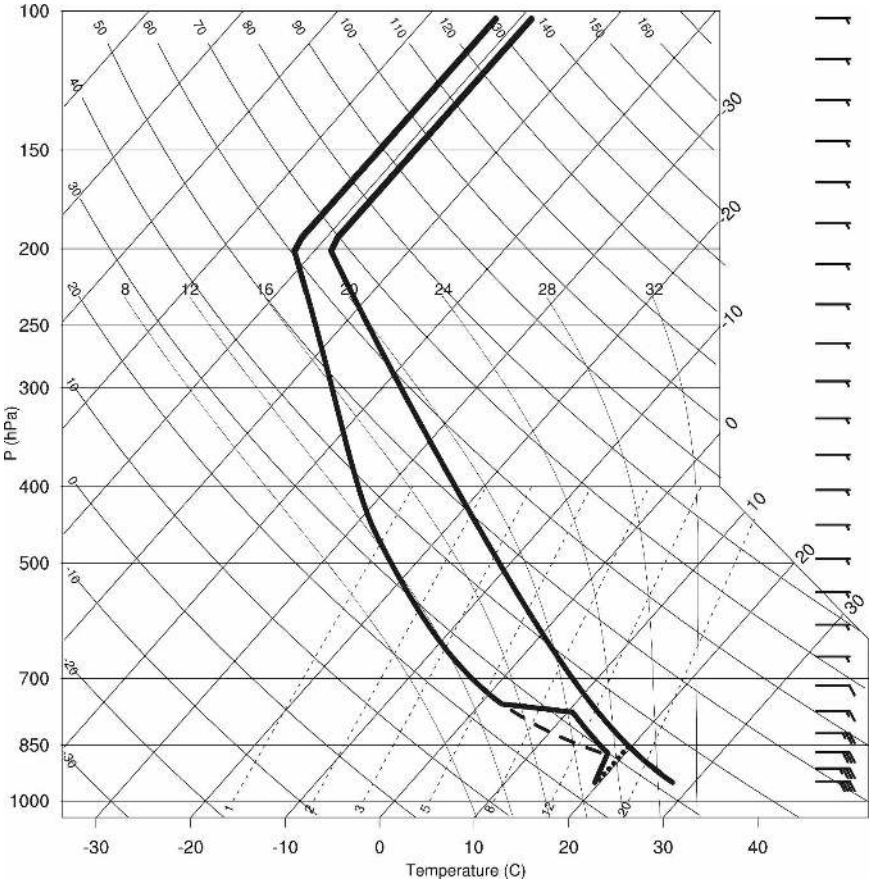

FIG. 1. Skew T–log$p$ diagram of the environmental soundings and storm-relative wind profile used in the numerical simulations: the DEEP initial sounding (solid), the PJ04 initial sounding (long dash), and the modified temperature sounding (dotted for both DEEP and PJ04) after the cooling in Eqs. (1)–(2) has been applied for 3 h. The WK82 sounding is not shown here (see WK82 for a depiction).

odic. The model had free-slip upper and lower boundaries with a Rayleigh damping layer above 14 km to minimize the impacts of reflections from the model top.

The simulations were meant to isolate the fundamental dynamical processes that govern convection on short time scales. Therefore, the model was configured in a highly idealized way, and mesoscale features such as fronts and low-level jets were excluded. The Coriolis acceleration was neglected, and the initial conditions were horizontally homogeneous. To initiate convection the model included an infinitely long, north–south, linear warm bubble (+2 K, with a relative humidity of 0.85); in the 3D simulations random temperature perturbations of up to 0.1 K were added to ensure that 3D motions developed.

All of the simulations used one of three idealized initial soundings: the convection sounding of Weisman and Klemp (1982, hereafter "WK82"); the mean midlatitude MCS sounding of Parker and Johnson (2004, hereafter "PJ04"), (Fig. 1, dashed); or the MCS sounding with a deeper moist layer from Parker and Johnson (2004), hereafter "DEEP" (Fig. 1, solid). The PJ04 sounding is of interest because it is representative of the mean environment for MCSs in the central United States and because it has very little moisture above the mixed layer (Fig. 1). Owing to this latter property, the most unstable parcels in the initial state reside in the lowest levels. As shown in Fig. 2, the PJ04 sounding is the only one among the soundings that has increasing CIN above the mixed layer; in addition, because of the dryness aloft, parcels above 750 m AGL must be lifted much farther in order to reach their LCL and LFC. These properties provide perhaps the most stringent test of the requirements for nocturnal convection and are representative of the dry, elevated mixed layers that are frequently present over the central United States.

The DEEP sounding, once cooled, is more akin to nocturnal soundings in which a low-level jet has fluxed

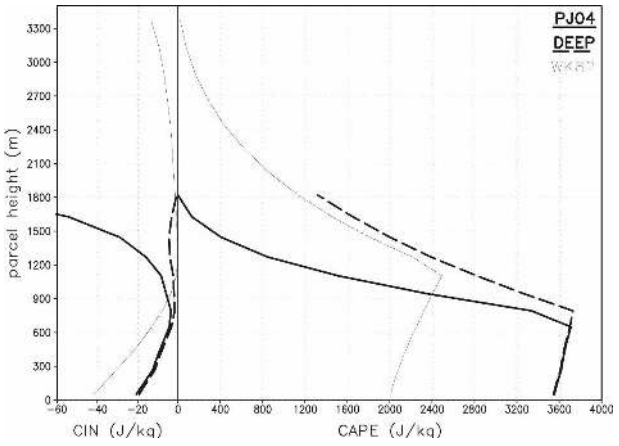

FIG. 2. CAPE and CIN for parcels at each level in the three initial soundings, using line styles as shown. For example, the surface parcel in the WK82 sounding has 2000 J kg^{-1} of CAPE and -40 J kg^{-1} of CIN. The curves are truncated at the level above which no other parcels have CAPE.

higher θ_e air into place above the boundary layer. Therefore, the working hypothesis was that the DEEP environment would better support elevated convection. The WK82 sounding was also used for the preliminary 2D experiments simply because of its prevalence in the history of convection simulations. Its basic lower-tropospheric properties are similar to the DEEP sounding; the principal difference is that it is moister in the middle and upper troposphere, which should slightly favor stronger, longer-lived storms. The control simulations had linear u wind shear totaling 18 m s^{-1} below 3 km, with constant wind above (e.g., Fig. 1); this is roughly the same shear vector magnitude as the preferred value for strong squall lines highlighted by Bryan et al. (2006).

Finally, the model included no boundary layer or radiative transfer parameterizations. Instead, it was pedagogically more valuable to add artificial cooling within some of the model runs. The cooling was added after three hours of simulated time (around the time when the simulated squall lines reached maturity). It was accomplished by defining a reference temperature

$$T_{\text{ref}} = 301 \text{ K} - (t - 3 \text{ h}) \times 3 \text{ K h}^{-1}, \quad (1)$$

and at each time step setting the temperature at all points below 1 km AGL to be

$$T = \min(T, T_{\text{ref}}). \quad (2)$$

The net effect was the creation of an isothermal layer whose temperature decreased from the initial surface temperature (301 K) at a rate of 3 K h^{-1}; because T decreased with height in the initial condition, the stable layer was initially shallow and grew slowly to its maximum depth of 1 km over the course of roughly 3 h (Fig. 1, dotted).

The artificial cooling technique is a simple way of enabling the convection to mature in an afternoon-like sounding and then to evolve as a nocturnal-like sounding develops. It might also represent the gradual transition experienced by a mature MCS crossing over to the cool side of a warm or stationary front. In various experiments, the cooling was applied until T_{ref} had reached between 280 and 291 K (net surface cooling between 10 and 21 K) in order to create stable layers of differing densities. Although, in reality, a fog would eventually form as the saturation vapor pressure decreased with T_{ref}, this was not well handled by the idealized microphysical parameterization. Therefore, when the artificial cooling was applied, the relative humidity was reset to be no larger than 0.98 through the instantaneous removal of water vapor (without any latent heat release).

As T_{ref} falls in time [Eq. (1)], the application of Eq. (2) causes the temperature difference between the outflow and the environment to decrease with time, as long as the outflow's temperature is lower than T_{ref}. Therefore, in order to isolate the possible importance of outflow strength versus environmental stability, an alternate cooling technique was also constructed (section 3d). The cooling to T_{ref} via Eq. (2) was applied between hours 3 and 5 of the simulation, after which all of the air below 1 km AGL was cooled at a constant rate of 3 K h^{-1} (including the convective outflow). This alternate configuration preserved the temperature difference between the outflow and the environment even as the boundary layer became increasingly stable.

Finally, in order to understand the response of low-level inflow air to the various imposed cooling profiles, passive tracers and massless parcels were inserted into the lowest 500–2500 m of the model domain and were integrated forward during the model time steps. The parcel trajectories were based on translation by the gridscale winds, whereas the passive tracers were also subject to the subgrid turbulent and numerical diffusion schemes. For all of the 3D runs that follow, the passive tracer was inserted in the 0–500-m AGL layer. Therefore, the presence of low-level air in convective updrafts can be inferred from the concentration of this tracer at midlevels.

3. Results

The early stages of this work involved a survey of over forty 2D simulations using the three initial soundings with multiple model configurations. There were

several preliminary sensitivity tests (not shown) that helped to qualify and guide the final control runs' configurations. First, in order to determine the ability of the environments to support convection that was totally decoupled from the near-surface air in the base state, pilot simulations used soundings with the lowest 1 km truncated (but with no cooling applied). In the "chopped" experiments, as anticipated, the WK82 and DEEP soundings supported long-lived convection, whereas the PJ04 sounding did not. The results for the three soundings were the same in "initial inversion" simulations, which had a 1-km-deep isothermal layer of 291 K (i.e., 10 K of surface cooling) present in the initial condition.

Once grounded by the preceding initial tests, the principal battery of 2D simulations permitted an assessment of the importance of the initial sounding to the behavior of the convection (WK82 versus PJ04 versus DEEP) when various amounts of lower-tropospheric cooling were applied. Most of the run-to-run sensitivities were similar for the various soundings, and the general impact of the cooling was the same in all three of the environmental soundings in the 2D simulation matrix. The robustness of the sensitivities within this pilot experiment provides some assurance that the results are not solely a function of the sounding used. Therefore, in order to complete the model runs in a reasonable amount of time, the 3D simulations focused on sensitivities within PJ04 and DEEP MCS environments. There was strong agreement between corresponding 2D and 3D runs. However, the following analyses of governing dynamics are based only upon the fully 3D simulations.

a. Control runs

The control simulations in both of the MCS environments (DEEP-ctl and PJ04-ctl) produced squall lines with evolutions typifying organized convection in the midlatitudes. The environments have ample CAPE, the vertical wind shear is appropriate for strong long-lived convective systems, and there is sufficient dry air aloft for the generation of cold downdrafts and surface outflow.

The two control simulations were very similar in character. The great resemblance of PJ04-ctl to DEEP-ctl stems from the identical wind profiles and low-level CAPE values (i.e., below 750 m AGL in Fig. 2). Both simulations produce a long-lived convective line (with trailing stratiform precipitation) that is cold pool driven and surface based. The supporting figures for this section depict the DEEP-ctl simulation in order to facilitate a more direct comparison with the other DEEP simulations reported in sections 3b and 3d. However, the discussion applies equally to the PJ04-ctl results, which are not depicted for brevity.

After 1 h in which the initial convective trigger leads to weakly organized storms, the systems' surface outflows begin to intensify. This initial stage will be referred to as "strengthening," because the systems' size and outflow temperature perturbations are increasing during the period. By the end of the stage, the systems' eastward motion commences, as is readily apparent from the Hovmöller diagram of updraft speed and tracer concentration aloft (middle panel of Fig. 3).

After roughly $t = 2$ h 30 min, the simulations' surface outflows have a nearly constant temperature deficit of roughly 14 K (left panel of Fig. 3). This second stage will be referred to as "quasi steady," because the systems' speeds and typical updrafts' strengths are roughly constant. Throughout this quasi-steady phase the systems' updrafts comprise air from the lowest part of the troposphere. The lifting of these low-level parcels is accomplished by the surface cold pool (Fig. 4d). As the systems move forward, the inflowing lower-tropospheric air is swept rearward over their cold pools (Figs. 4b,c), leading to the development of trailing stratiform precipitation (Figs. 4a,b).

Although the 3D simulations were halted after 8 h, in 2D the systems remain quasi steady for as long as the simulations run. Based upon outflow temperature and system motion speed, the period of quasi-steady behavior begins sometime between 2 and 3 h into the simulation. Therefore, the experiments with artificial low-level cooling were configured to allow the convective systems to develop for 3 h, after which the model environment was slowly modified. In this configuration, any subsequent changes in system speed, cold pool temperature, tracer concentration, or the like are therefore attributable to modifications of the environment, not to the maturation of the squall line itself.

b. Addition of unlimited cooling

Given that simulations using the initial inversion and "chopped" versions of the PJ04 sounding did not produce long-lived convective systems, it is not surprising that, when unlimited cooling is introduced into the model (i.e., T_{ref} is allowed to decrease indefinitely), the simulated PJ04-unlim squall line decays into a very weak and disorganized precipitation system (not shown). By $t = 10$ h, it bears no resemblance to the mature squall lines in the control runs. However, a weak but organized convective system does survive when *limited* cooling is applied to the PJ04 simulations. Thus, the PJ04 simulations are set aside for now and are explored in the next section. The following results are from the DEEP sounding for the case of unlimited

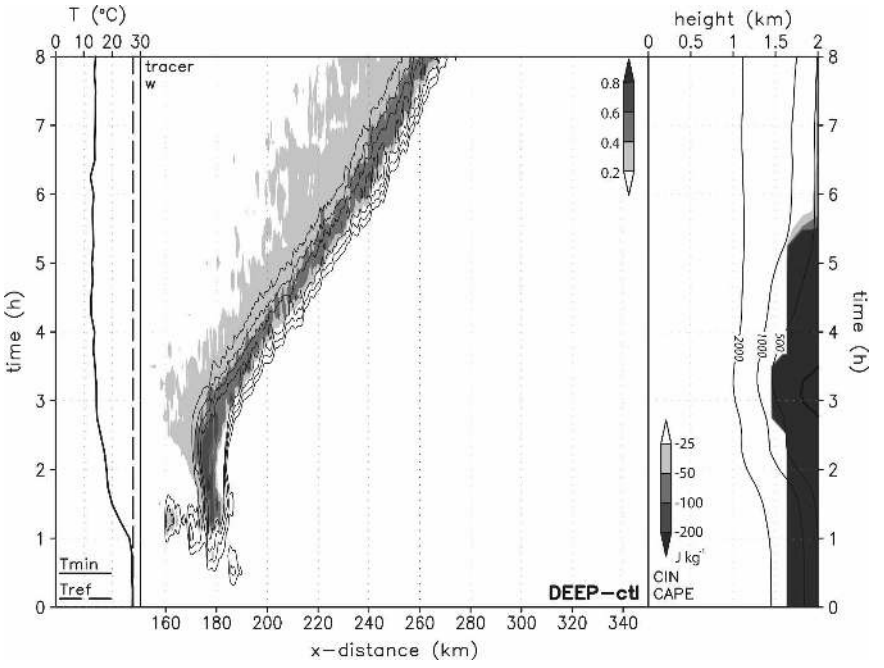

FIG. 3. Depiction of the DEEP-ctl simulation over time: (left) values vs time for the reference temperature used in Eq. (2) (T_{ref}) and the minimal surface temperature on the domain (T_{min}), using line styles as shown; (center) Hovmöller diagram for 5 km AGL, with along-line maxima in tracer concentration (shaded as shown) and vertical velocity (contoured at 10, 15, 20, and 25 m s^{-1}); (right) vertical profile of environmental CIN (shaded as shown) and CAPE (contoured at 500, 1000, and 2000 J kg^{-1}, with bold contour at 0) vs time. The ordinate for all three panels is the same (time).

cooling. Because the DEEP sounding has elevated parcels with CAPE, it remains healthy and well organized through the full 10-h simulation. The DEEP-unlim system's transition from a surface-based to an elevated system is therefore more instructive because it is not simultaneously disintegrating.

The first three hours of the DEEP-unlim run are identical to those of the DEEP-ctl run with the system passing through the strengthening stage and into the quasi-steady stage (cf. Figs. 3 and 5). Once cooling is applied below 1 km after t = 3 h, the lower-tropospheric CAPE begins to decrease (right panel of Fig. 5), and the cold pool's temperature deficit (relative to the environment) begins to diminish (Fig. 5). Despite these facts, the system's middle-tropospheric updraft speeds and tracer concentrations are very similar to those in the control run through roughly t = 5 h 30 min. Although the two simulations are not identical, it is fair to say that the addition of roughly 7–8 K of surface cooling has relatively little impact, and the DEEP-unlim simulation continues to exhibit its quasi-steady behavior. Notably, because the cooling via Eqs. (1) and (2) creates an increasingly deep isothermal layer, it takes time before the CAPE farther aloft decreases (Fig. 5).

From roughly t = 5 h 30 min to 7 h 30 min, the DEEP-unlim system then enters a third stage that is not exhibited by the DEEP-ctl simulation. The system's speed decreases as the environment's temperature begins to approach that of the convective outflow; hence, the period will be referred to as "stalling" (Fig. 5). That the updraft forcing is still driven by density current dynamics is apparent from a cross section of potential temperature (Fig. 6d), as well as the upward displacement of all inflow parcels at the gust front (Figs. 6b,c). The slowing of the cold-pool-driven system is in keeping with the basic dynamics of density currents, whose speeds are proportional to the square root of the temperature difference across the outflow boundary. As shown in Fig. 7, the system's speed is not quite as large as the theoretical density current speed[1]; but, the trend

[1] The speed of the system's outflow may be diminished because of the quasi-static impacts of positively buoyant air aloft (as discussed by Trier et al. 2006) as well as by the opposing low-level vertical wind shear. However, Bryan and Rotunno (2008) have also reviewed other theoretical reasons why the classical density current speed may overestimate the motion of realistic atmospheric density currents.

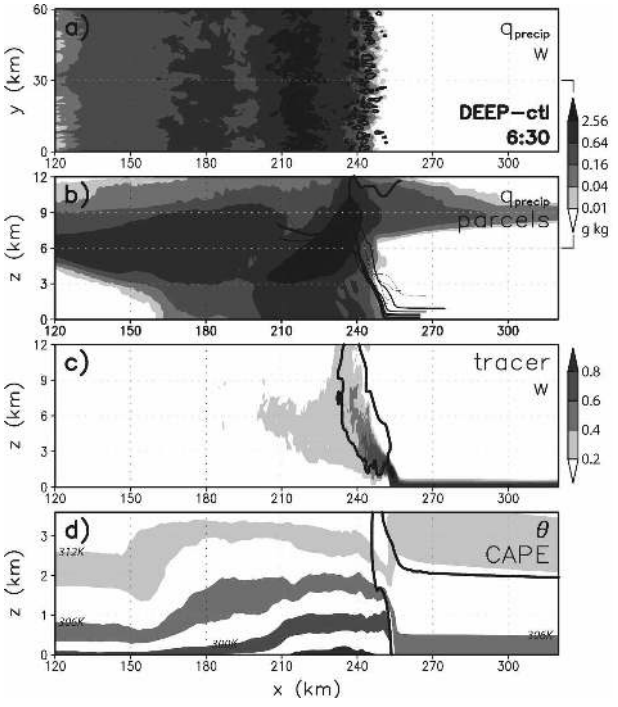

FIG. 4. Depiction of selected fields at $t = 6$ h 30 min of the DEEP-ctl simulation: (a) plan view of 1–6 km AGL mean precipitation mixing ratio (shaded as shown) and 5 km AGL vertical velocity (contoured at 10 m s^{-1}); (b) vertical cross section of along-line averaged precipitation mixing ratio [shaded as in (a)] and 1-h-long run time parcel trajectories from the simulation, centered at $t = 6$ h 30 min; (c) vertical cross section of along-line maxima in tracer concentration (shaded as shown) and vertical velocity (contoured at 10 m s^{-1}); (d) vertical cross section of along-line averaged potential temperature (alternately shaded every 3° across the lowest 18 K, from dark to light, starting at 294 K) and CAPE (contoured at 500 J kg^{-1}). The abscissa for all four panels is the same (x). Note that the ordinate varies among panels.

in the system's speed follows the trend in the idealized density current speed. The decrease in speed alone may be of little concern, but the relative decrease in the cold pool's strength also has a dramatic impact upon system strength.

Between hours 3 and 6 there is a general trend toward decreasing total updraft mass fluxes. This is partly attributable to the decrease in environmental CAPE and partly due to the fact that inflowing air parcels are generally being swept rearward over the outflow. However, during the stalling phase this decrease is curtailed and there is a brief period of increasing total updraft mass fluxes; the DEEP-unlim system tends toward stronger updrafts (Figs. 5 and 6a,c), more upright parcel trajectories (Figs. 6b,c), and higher tracer concentrations aloft (Figs. 5 and 6c). These properties attain their secondary maximum around $t = 6$ h 30 min. The stalling phase of the DEEP-unlim simulation is not actually stronger than the DEEP-ctl system, no doubt because the low-level CAPE has decreased so much. However, it is notable that the DEEP-unlim case produces strong surface-based convection during the stalling phase even as CAPE in the lowest half kilometer is waning and CIN is increasing (Fig. 5). The trajectories and the shape of the tracer field are quite similar to those of the DEEP-ctl run during this stage (cf. Figs. 4 and 6).

According to the work of Rotunno et al. (1988), often called "RKW theory," gust front lifting and updraft strength for cold-pool-driven systems should be maximized when there is an approximate balance between the line-perpendicular environmental vertical wind shear and the horizontal vorticity that is generated baroclinically at the outflow boundary. Rotunno et al. (1988) and Weisman and Rotunno (2004) cast this in terms of the unitless ratio between the cold pool's theoretical density current speed (C) and the total change in the line-perpendicular wind (ΔU) over some lower-tropospheric layer; their claim was that the optimal ratio for deep gust front lifting is $C/\Delta U \approx 1$. The appropriate depth and vertical distribution for ΔU is not always clear (e.g., Weisman and Rotunno 2004), and the optimal ratio itself can be a moving target because cold pool strengths are themselves a function of the magnitude of the shear (e.g., Stensrud et al. 2005). Even so, a wide variety of numerical experiments with a wide variety of numerical models (e.g., Bryan et al. 2006) have supported the basic tendencies in system strength and structure that are predicted by RKW theory. As shown in Fig. 7, the stalling phase is one in which the cold pool strength (measured either in terms of integrated buoyancy or in terms of the system's forward speed) decreases toward the optimal ratio of 1. This largely offsets the increasing CIN and decreasing CAPE of the parcels that are being lifted, such that the stalling system remains surface based.[2]

Between 6 h 30 min and 7 h, two processes combine to cause the end of the surface-based stage of the DEEP-unlim system. First, CAPE in the lowest 500 m decreases from roughly 500 to 0 J kg^{-1}(with CIN be-

[2] An alternative hypothesis for the reintensifying convection is that, as the gravity wave and density current speeds approach one another (Fig. 7), there is a resonance or accumulation of the two lifting mechanisms. However, in the DEEP-unif simulation (section 3d), wherein the cold pool remains strong, there is no secondary reintensification when the gravity wave speed approaches the density current speed (i.e., the lack of a secondary maximum in Fig. 15). In short, the cold pool's declining strength appears to be the key.

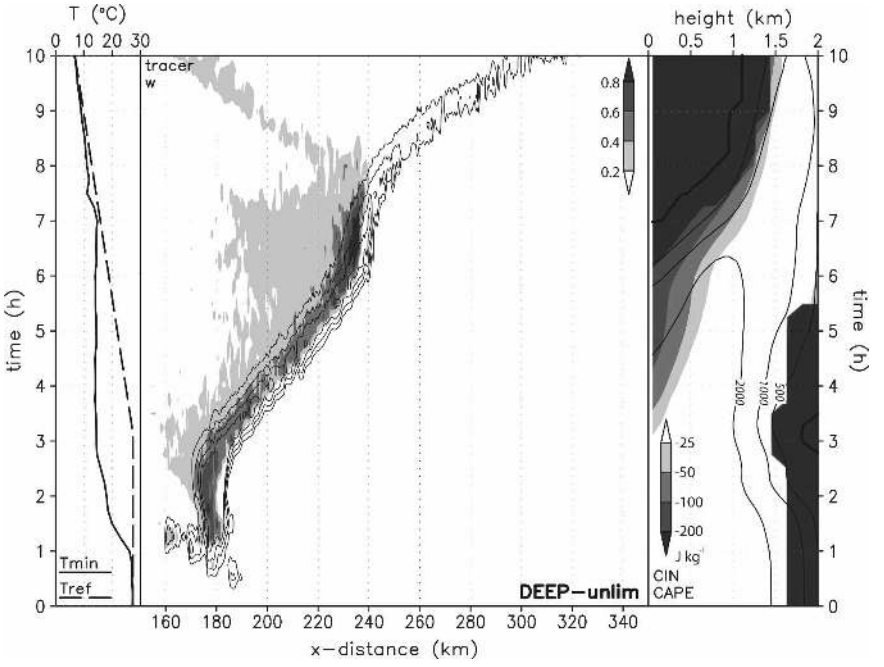

FIG. 5. As in Fig. 3 except for the DEEP-unlim simulation.

coming increasingly negative as well; Fig. 5). This alone would be sufficient to eliminate the low levels as a source of parcels for deep convection. In addition, however, the cold pool's relative strength tends toward zero during this time as well (Fig. 5). In other words, the mechanism for lifting low-level parcels begins to disappear. Shortly thereafter (some time between 7 h and 7 h 30 min), these factors therefore lead to the fourth and final stage of the DEEP-unlim system, here deemed the "elevated" stage.

During the elevated stage, tracer concentrations in the middle troposphere go to zero, indicating a lack of low-level air in the convective updrafts (Figs. 5 and 8c). Instead, the low-level parcels embody an "underflow" regime, in which the inflow air experiences very little vertical displacement, and predominantly flows rearward along the surface. Trajectories (Fig. 8b), tracers (Fig. 8c), and other approximately conserved variables (e.g., θ_e, not shown) all reveal that parcels in the stable boundary layer pass directly underneath the deep convection without participating in it. As well, updraft speeds diminish (Fig. 5, and cf. Figs. 6a,c and 8a,c). This weakening of the deep convection is a symptom of decreasing CAPE with time (e.g., in the 500–1000 m AGL layer, see Fig. 5, which subsequently feeds the elevated convection) and it is also a symptom that the deep cold-pool-driven lifting of the stalling stage is no longer present. Finally, the system's forward speed changes dramatically during the transition from the stalling to the elevated stage. Indeed, toward the end of the simulation, the DEEP-unlim system moves at a faster speed than at any other time during the simulation (Fig. 7). This is associated with a new forcing mecha-

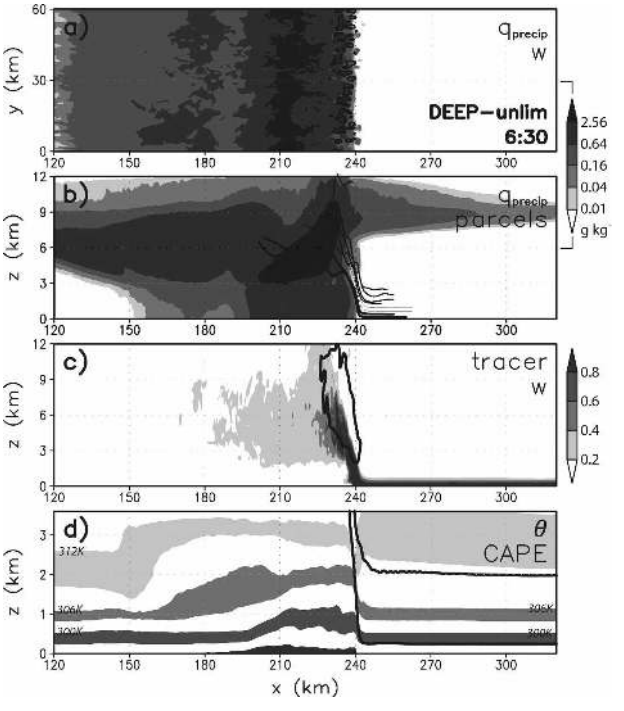

FIG. 6. As in Fig. 4 except for the DEEP-unlim simulation at t = 6 h 30 min.

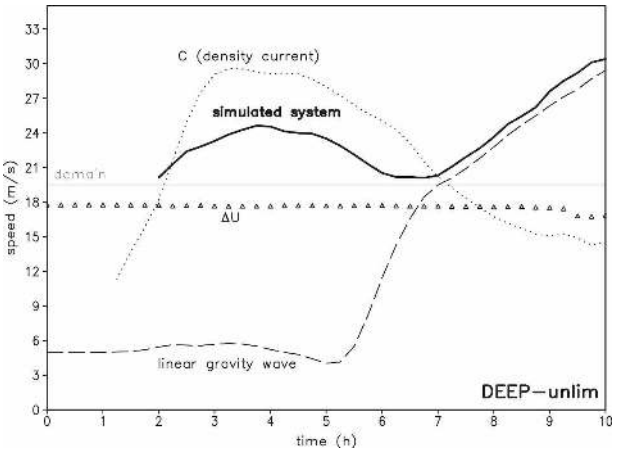

FIG. 7. Evolution over time of speeds relevant to the motion and intensity of the simulated DEEP-unlim system. The actual simulated system's speed, as inferred from motion of the gust front, is in bold. The theoretical density current speed for the surface outflow, C (dotted), is computed following the method of Weisman and Rotunno (2004) and Bryan et al. (2006). The actual and density current speeds are not plotted until a well-established gust front or density current is apparent. The theoretical linear gravity wave speed (dashed) is computed using the buoyancy frequency one grid point above the 1-km-deep layer of cooling, and a vertical wavelength of 6.5 km (based on the p' field in Fig. 9). For reference in discussions of the outflow strength relative to the vertical wind shear, the magnitude of the 0–3-km vector wind difference (ΔU) is indicated with triangles. Note that the domain moves eastward at 19.2 m s^{-1} (thin horizontal line), rendering much smaller grid–relative speeds in the system's Hovmöller diagram (Fig. 5).

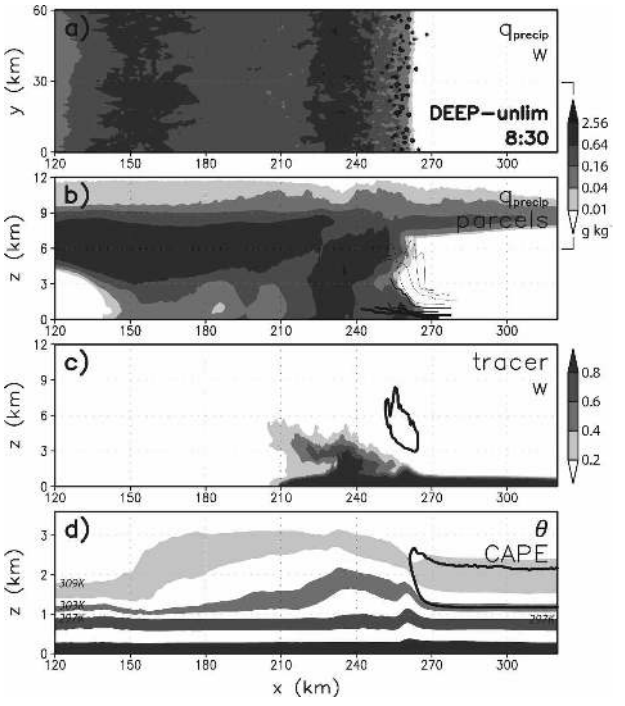

FIG. 8. As in Fig. 4 except for the DEEP-unlim simulation at t = 8 h 30 min. First (darkest) θ contour in (d) is at 291 K.

nism;[3] elevated convection in this case is sustained by lifting via a propagating internal bore. That the new lifting mechanism is a bore is evident in the sudden deepening of the low-level stable layer as it passes through the convective region, seen in both the tracer and potential temperature fields (Figs. 8c,d). The bore is attended by a cold anomaly that originates as a part of the preexisting cold pool's head and is subsequently maintained as a result of parcels that have ascended within the bore's deepened stable layer. The region of increased depth also has decreased front-to-rear velocity ($u' > 0$; Fig. 9a). These perturbations in depth, u, and θ extend on the order of 100 km rearward from the gust front, in keeping with the conventional definition of a bore as a "semipermanent" jump in the fluid. Inflowing air passes characteristically *through* the bore, constituting the underflow regime.

As the low-level cooling begins, the outflow density current is supercritical; in other words, at first the density current's speed exceeds the intrinsic speed of internal gravity waves for the preline layer (Fig. 7). Rottman

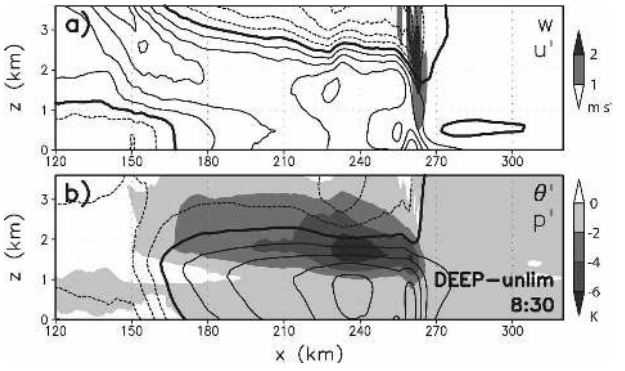

FIG. 9. Depiction of additional fields at t = 8 h 30 min of the DEEP-unlim simulation: (a) vertical cross section of along-line averaged vertical velocity (shaded at 1 and 2 m s^{-1}) and perturbation line-perpendicular wind (contoured every 3 m s^{-1}, with bold contour at 0, negative values dashed), and (b) vertical cross section of along-line averaged potential temperature perturbation (shaded as shown) and pressure perturbation (contoured every 50 Pa, with bold contour at 0, negative values dashed). Note: these perturbations are relative to the cooled environment at t = 8 h 30 min; the surface air beneath the convective system is no longer cooler than the preline air, so θ' is minimal below 1 km AGL. The abscissa and ordinate for both panels is the same.

[3] There is another small effect due to the system's decoupling from the 0–1-km layer, which increases the 0–6-km mean wind by roughly 2 m s^{-1}. However, this small increase is not sufficient to explain the increase in system speed or its ongoing upward trend (shown in Fig. 7).

and Simpson (1989) note that, when a shallow layer of stable fluid is encountered by a supercritical density current, the typical result is a "type C" bore, whose speed is the same as the density current driving it and whose properties are very similar to density currents. This regime prevails in the DEEP-unlim simulation through roughly $t = 5$ h. As the preline cooled air becomes comparable in depth to the density current but the outflow air is still colder than the environmental air, the situation becomes akin to a lock release problem in which a denser fluid intrudes into a slightly less dense fluid of comparable depth (e.g., Fig. 7 of Rottman and Simpson 1989; cf. Fig. 6d herein). Finally, as the continuing cooling causes the preline air to be the same temperature as the outflow air, the situation becomes akin to a simple internal bore (e.g., Fig. 1 of Klemp et al. 1997; cf. Fig. 8d herein) in which the stable fluid depth abruptly changes across a jump at which there is no appreciable density discontinuity. According to theory (e.g., Fig. 8 of Klemp et al. 1997), in such a scenario the speed of the bore (and hence the convective system) tends toward the gravity wave speed as the prebore stable layer's depth is increased. This evolution of outflow from density current dynamics to gravity wave dynamics is similar to what Carbone et al. (1990) and Knupp (2006) observed.

The perturbation wind, potential temperature, and pressure fields during the elevated, bore-driven stage (Fig. 9) suggest that the propagation of the bore is through a gravity-wave-like process, with a quasi-static pressure maximum in the stable layer (Fig. 9b), and an in-phase maximum in the rear-to-fore wind perturbation (Fig. 9a), beneath the cold anomaly in the head of the bore (Fig. 9b). The forward speed of the convective system after roughly $t = 7$ h (Fig. 7) is also very close to the theoretical speed for linear gravity waves (e.g., Holton 2004). As the low-level stability increases, so does the gravity wave speed and, hence, the system's speed (Fig. 7). Even as the convection weakens (after 8 h in Fig. 5) the system's rapid motion is maintained, principally because the gravity wave speed is not a function of the wave amplitude.

In keeping with the findings of Raymond and Rotunno (1989), the bore's gravity-wave-like forcing does not take over until it becomes faster moving than the original cold pool forcing (Fig. 7). This occurs in the later part of the stalling phase, when there is negligible remaining surface temperature gradient across the gust front and the pre-gust-front environment constitutes a deep layer of high stability. Of course, as mentioned previously, this is also around the time that the surface-based CAPE vanishes. But, the bore's forcing appears to take over around $t = 7$ h (based on the change in system motion), which is before the 0–1-km layer is completely devoid of CAPE (*some* parcels below 1 km retain CAPE > 0 J kg^{-1} through 8 h, Fig. 5). The experiment in section 3d revisits in more detail the possible roles of CAPE versus the forcing mechanism.

The fact that convection in the DEEP-unlim simulation can survive for an additional 3+ h without low-level CAPE is a somewhat novel result. The transition through the strengthening, quasi-steady, stalling, and elevated stages occurred in an environment with increasing low-level stability (such as would occur during the late afternoon and evening). Furthermore, the elevated convection was sustained without the presence of a low-level jet, synoptic-scale front, or other horizontal heterogeneity. In the present case, the mechanism for maintenance is a propagating bore atop the imposed stable layer. If a surface-based storm can be initiated, then there is an intrinsic process for sustaining storms as the boundary layer cools (e.g., at night). An interesting result is that, just before the transition to the elevated state, the system experiences a brief window of intensification as the cold pool's temperature deficit decreases with respect to the preline environment.

c. *Addition of limited cooling*

Having learned from the DEEP simulations, which have appreciable elevated CAPE, it becomes worthwhile to return to the PJ04 environment. As mentioned above, the squall line in the PJ04 environment dwindled into an unorganized, weak precipitation system before the end of the 10-h simulation when unlimited cooling was applied. This sounding is the only one among the three that has minimal CAPE for parcels above the lowest 1 km (due to the sounding's dryness aloft, Fig. 2). It is therefore instructive to explore the fundamental processes within the PJ04 environment after intermediate amounts of cooling. How much cooling is needed in order to cut the system off from its supply of near-surface air?

In the first experiment, T_{ref} was only allowed to decrease by 10 K, to 291 K ("PJ04-291K"). The system in the stabilized environment continues to produce strong updrafts, and remains surface based (Fig. 10). It continues to have a temperature gradient across the outflow's leading edge, and the low-level tracers are all lifted abruptly at the outflow boundary (not shown). In short, the initial 10 K of surface cooling applied between 3 and 6 h does not hinder the squall line much.

Although the net 10 K surface cooling may not be as large as the full nocturnal temperature range on many evenings, it is sufficient to appreciably increase the surface-based CIN and to remove most of the surface-based CAPE (Fig. 10). Despite this fact, the convec-

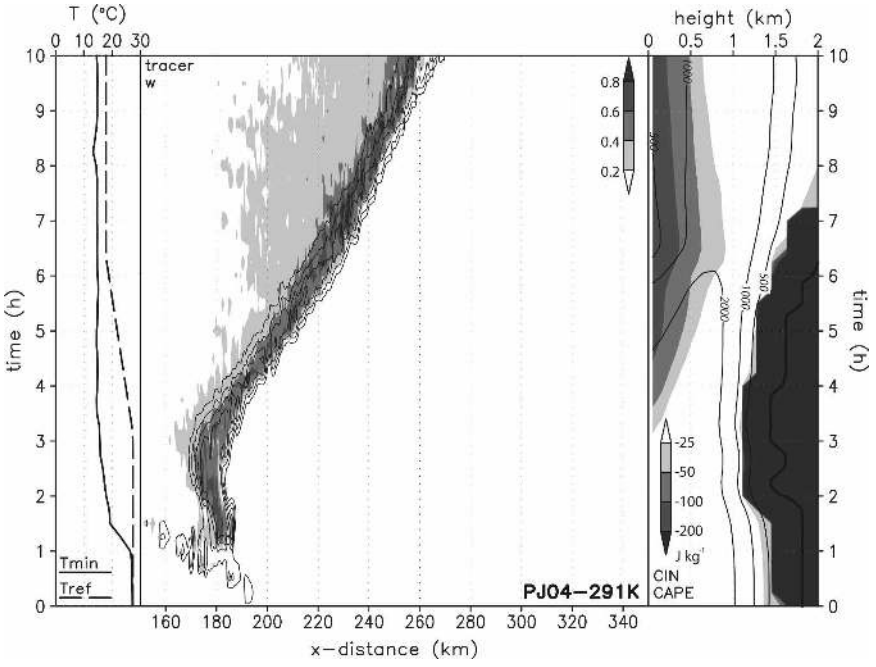

FIG. 10. As in Fig. 3 except for the PJ04-291K simulation.

tively generated cold pool remains and is sufficient to lift air parcels to their LFCs. In fact, an interesting result is that the updraft strength and tracer concentrations in the middle troposphere remain almost constant with a slight increase after several hours of cooling, much as was observed during the stalling phase of the DEEP-unlim simulation.

A cursory examination of the environment after $t =$ 6 h, with its highest CAPE values aloft (Fig. 10), might give the mistaken impression that the convection is elevated. However, because the near-surface parcels continue to possess CAPE and because the cold-pool-driven lifting persists (and even intensifies), the PJ04-291K simulation produces a long-lived, surface-based convective system. This result has several implications. First, a substantial amount of cooling (for the PJ04 sounding, more than 10 K) is needed in order to cut off the low-level inflow stream of a mature convective system. And second, if a cold pool of convective outflow can be established before boundary layer stabilization ensues, then the cold-pool-driven lifting can overcome surprising amounts of CIN, as long as there is some CAPE remaining. Taken together, the results suggest that *many of the nocturnal convective systems that were previously thought to be elevated may actually be surface based*.

In the next experiment, T_{ref} was allowed to decrease by 12 K to 289 K ("PJ04-289K"). This second simulation is identical to the PJ04 291-K simulation through 6 h 20 min, after which it begins to diverge due to the additional cooling that is applied between 6 h 20 min and 7 h. Through 7 h of simulation, however, the gross behaviors are the same in the 291-K and 289-K simulations (cf. Figs. 10 and 11). The updraft speeds and tracer concentrations increase slightly as the cold pool's temperature perturbation weakens (Fig. 11). Differences become evident after 7 h, however. The PJ04-289K convective system continues sporadically to ingest some near-surface air, and its updrafts remain strong (peaking above 20 m s^{-1}, Fig. 11). However, the midlevel concentration of tracer is clearly much lower than in the 291-K simulation, and than in the earlier stages of the 289-K simulation (Figs. 11, 12c).

At the system's leading edge, a very weak cold pool persists with a temperature deficit of roughly 1 K (not visible given the contour interval in Fig. 12d). However, the surface parcels now have no CAPE (Fig. 11), and the parcels around 500 m AGL have very little CAPE ($\leq$500 J kg^{-1}; Figs. 11, 12d), along with CIN of roughly -150 J kg^{-1}. In other words, many of the parcels in the lowest 500 m have no LFCs, and those that do require appreciable lifting. But, in the lower troposphere the surfaces of potential temperature are nearly horizontal (Fig. 12d), implying only small vertical excursions for the low-level parcels. A quasi-static pressure maximum remains as a result of the pocket of outflow air aloft (above the cooled layer) such that the inflowing near-surface air parcels are slowed on passing through the

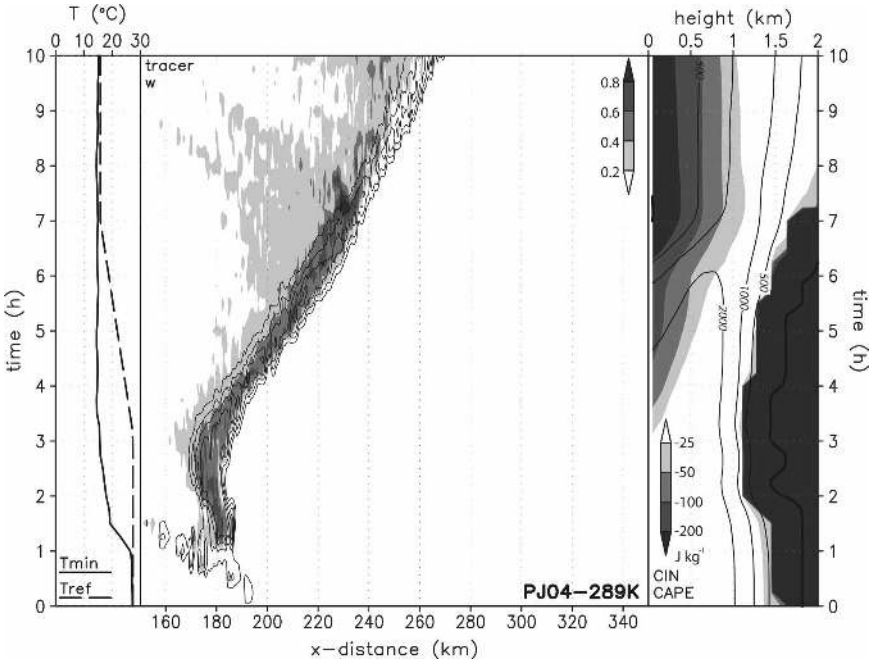

FIG. 11. As in Fig. 3 except for the PJ04-289K simulation.

gust front (not shown). The net result is a localized region in which the layer of 0–500-m inflowing parcels collect and weakly ascend (Fig. 12c). However, the LFCs for these parcels are either quite high or nonexistent, so very few become positively buoyant. Those that do typically have rather shallow total displacements (Fig. 12b), because their CAPE is small, and they begin to constitute the lower and middle levels of the simulated convective system's trailing stratiform precipitation region. The air parcels feeding the strong, deep updrafts are from farther aloft (i.e., above 500 m AGL, Fig. 12b). In short, the PJ04-289K simulation represents a quasi-steady, long-lived system that sits right on the threshold between being surface based and elevated.

In the third PJ04 experiment, T_{ref} was allowed to decrease by 14 K to 287 K ("PJ04-287K"). This run is of particular interest because 287 K is the approximate temperature of the near-surface outflow air in the PJ04 control simulation. The PJ04-287K simulation is identical to the PJ04-289K simulation through 7 h, after which it begins to diverge due to the additional cooling that is applied between 7 h and 7 h 40 min. After 7 h 40 min, the surface outflow is no longer colder than the cooled preline environment because T_{ref} has reached the outflow temperature (Fig. 13).

The PJ04-287K simulation exhibits one symptom of the "stalling" phase, in that it has a brief secondary maximum in midlevel updraft strength and tracer concentration around $t = 7$ h 30 min (Fig. 13). But, unlike in the DEEP-unlim simulation, the system's speed decreases by only a few meters per second. Descending air from the system's rear inflow jet adds to the system's

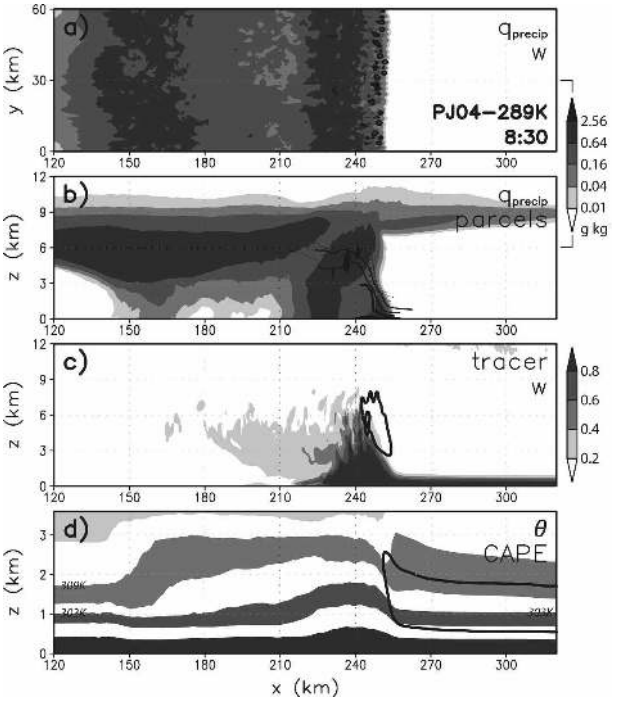

FIG. 12. As in Fig. 4 except for the PJ04-289K simulation at $t =$ 8 h 30 min. The first (darkest) θ contour in (d) is at 297 K.

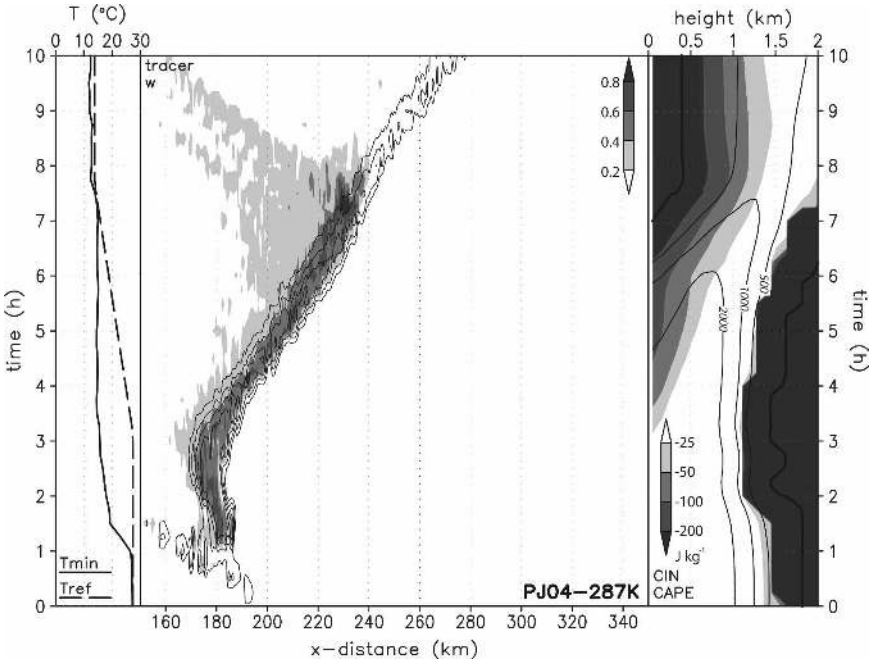

FIG. 13. As in Fig. 3 except for the PJ04-287K simulation.

forward speed during this time frame (not shown). A rear inflow jet is also present aloft in the DEEP-unlim simulation, but it does not descend to the surface. However, because the surface cold pool is slightly warmer on average in the PJ04-287K simulation, and because there is additional evaporative cooling within the rear inflow jet due to the dry air aloft, the higher momentum parcels are able to descend all the way to the surface in the PJ04-287K simulation. This partly offsets the decline in cold pool temperature deficit during the PJ04-287K system's stalling phase.

The PJ04-287K convective system is clearly elevated after roughly 8 h, and remains so through the rest of the simulation (Fig. 13). The additional cooling leaves very few parcels with nonzero CAPE in the lowest 1 km of the environment (Fig. 13). Those that do have some small amount of remaining CAPE (above about 800 m AGL, with CAPE values between 0 and 300 J kg^{-1}) also have large magnitudes for CIN (from -100 to -350 J kg^{-1}). Whereas such CIN values were not problematic for the strong cold pool in the PJ04-291K simulation, the excess cooling in the PJ04-287K simulation leads to potential temperature surfaces that have almost no slope, especially in the lowest few hundred meters AGL (not shown).

How is it that the PJ04-287K convection can survive as an elevated system when it is apparently feeding on the dry layer of air aloft? Figure 13 reveals that moderate values of CAPE are found at increasingly higher heights during the later stages of the simulation: at 1.8 km AGL, the initial condition has no CAPE, but the environment at $t = 10$ h has CAPE ≈ 500 J kg^{-1}. Model animations show the presence of low-frequency tropospheric internal gravity waves that propagate ahead of mature convective systems and modify the preline environment, just as discussed by Nicholls et al. (1991), Mapes (1993), Fovell (2002), and others.

In the far field, the first signal to arrive is a quickly propagating wave of deep-tropospheric subsidence; this signal represents a response to the deep-tropospheric heating profile within the convective region of a simulated MCS. Such subsidence impacts the preline environment of the PJ04-287K simulation through roughly the first 3 h (Fig. 14a), and can be seen to displace surfaces of θ_e downward. Thereafter, a second signal arrives: a more slowly propagating wave of lower-tropospheric ascent. As explained by authors such as Nicholls et al. (1991), Mapes (1993), and Fovell (2002), this wave is a response to parts of the squall line's diabatic heating/cooling profile with shorter vertical wavelengths (especially low-level cooling). As a result, the θ_e surfaces are displaced upward after roughly $t = 3$ h 30 min (Fig. 14a) with low-level parcels eventually exceeding their initial heights. This later-arriving wave of ascent adds CAPE and removes CIN, enabling tropical convection to be "gregarious" in the conceptual model of Mapes (1993) and accounting for the primed "cool/moist tongue" of Fovell (2002). These effects are com-

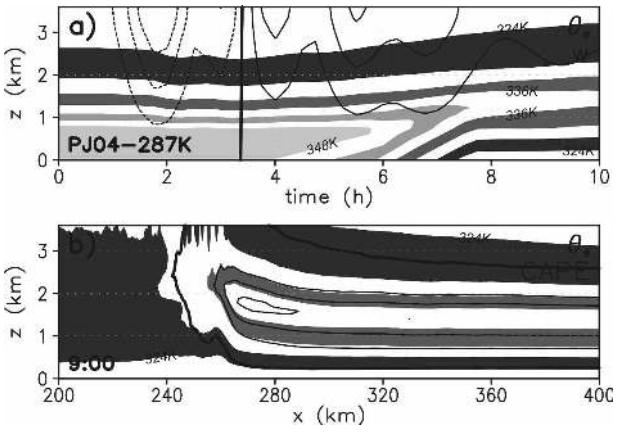

FIG. 14. Equivalent potential temperature (θ_e) and related fields for the PJ04-287K simulation: (a) profile vs time of mean environmental θ_e (alternately shaded from dark to light every 4°, from 324 to 348 K) and vertical velocity (contoured from −0.06 to 0.06 m s^{-1}, every 0.02 m s^{-1}, with bold contour at 0, negative values dashed); values are for the far field (along the eastern domain edge); and (b) vertical cross section at t = 9 h of along-line averaged θ_e [shaded as in panel (a)] and CAPE (contoured at 250, 500, and 750 J kg^{-1}, with bold contour at 0).

mon to all of the present simulations and can be seen in Figs. 3, 5, 10, 11, 13, and 15; the symptoms are the decrease and rebound of the CAPE values above roughly 1 km AGL between t = 0 and 6 h and the subsequent disappearance of CIN above 1.5 km AGL after approximately t = 5.5–7 h. In short, the low-frequency waves are partly responsible for the presence of higher θ_e parcels above the 0–1-km layer of artificial cooling. Because the preline air is closer to its LCL and LFC, relatively less lifting is then needed in the convective region.

A second effect also supplements the environmental CAPE in the immediate vicinity of the convective region. As shown in Fig. 14b, θ_e decreases with height above its maximal value at roughly 1.3 km AGL. In other words, the inflow above the stable layer has little CAPE but it is potentially unstable. Lifting in the immediate vicinity of the propagating bore (i.e., between x = 260 and 280 km in Fig. 14b) realizes some of this potential instability. The inflowing layer is slightly destabilized and CAPE values increase, exceeding 750 J kg^{-1} just as the parcels enter the convective region. The PJ04 sounding is representative of many MCS environments in the central United States, which often possess a dry, elevated mixed layer. Therefore, θ_e decreases with height on many convective days, and the conversion of potential instability by lifting at the convective system's leading edge becomes yet another viable ingredient for the sustenance of convection as nocturnal cooling ensues.

d. *Unlimited uniform cooling*

The preceding analyses suggest that there are two critical components in the maintenance of a convective system as the lower troposphere is stabilized. First, air

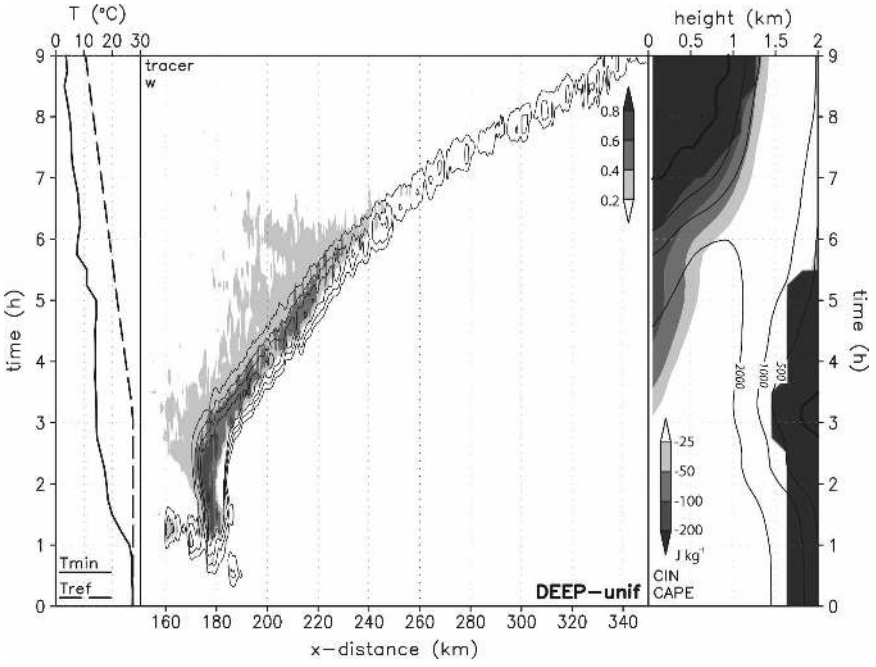

FIG. 15. As in Fig. 3 except for the DEEP-unif simulation.

parcels must exist with CAPE and, second, there must be a dome in the isentropes, whether in the form of a surface-based cold pool or a bore atop the stable layer, that is capable of lifting the parcels with CAPE to their LFCs. With low-level cooling, surface-based cold-pool-driven systems evolve to become elevated, bore-driven systems. However, one artifact of the artificial cooling in the above experiments is that the CAPE of near-surface air disappears at roughly the same time that the outflow's near-surface temperature perturbation disappears. The following test isolated the role of the cold pool versus the role of CAPE by cooling the outflow at the same rate as the environment after five simulated hours. In other words, cooling is applied according to Eq. (2) from 3 to 5 h in the following runs, after which every grid point below 1 km AGL is cooled at a rate of 3 K h^{-1}. Therefore, the outflow's temperature perturbation remains the same after 5 h.

The result was somewhat surprising. Updrafts in the uniform cooling ("unif") experiments weaken and became elevated much earlier than in the unlimited cooling ("unlim") experiments (again, only the results from the DEEP environment are shown, Fig. 15). As well, despite removal of environmental CAPE at an identical rate, the PJ04-unif convective system dies before completion of eight simulated hours (not shown), almost two full hours sooner than in the PJ04-unlim experiment. Several differences from the "unlim" simulations are apparent.

Neither the PJ04-unif nor the DEEP-unif simulations experienced the stalling phase, with its reintensified updrafts. Because the outflow's temperature deficit remained constant, both the PJ04-unif and DEEP-unif systems moved at constant speed through roughly $t = 6$ h 30 min. Thereafter, as the gravity wave speed exceeded the density current speed, the systems began to accelerate (e.g., Fig. 15). Indeed, the DEEP-unif simulation had to be stopped after 9 h because the convection so quickly approached the eastern lateral boundary.

The "uniform" cooling also prevents the outflow from returning to a condition that is more nearly in balance with the environmental shear. This has several effects. First, there is no secondary maximum in deep lifting as was observed in the other cooled simulations (sections 3b and 3c, cf. Figs. 5 and 15) and, second, because the lifting of near-surface air is far from optimal in the uniform cooling experiments, the simulated systems become elevated more rapidly (cf. Figs. 5 and 15). In other words, despite the same chronology of environmental CAPE and CIN, the convective systems in uniform cooling are much sooner unable to get near-surface parcels to their LFCs.

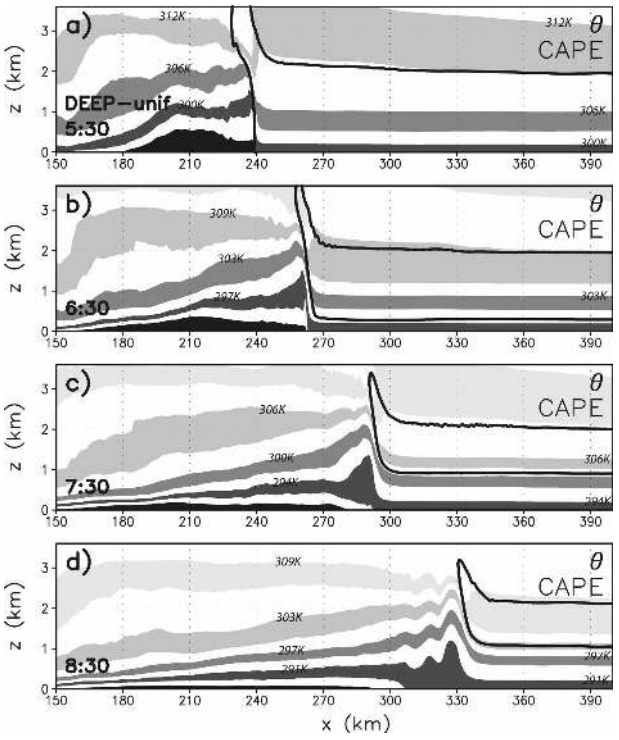

FIG. 16. As in Fig. 4d except for the DEEP-unif simulation at times (a) $t = 5$ h 30 min, (b) $t = 6$ h 30 min, (c) $t = 7$ h 30 min, and (d) $t = 8$ h 30 min. The contour levels change among panels. Potential temperature is alternately shaded every 3° across the lowest 24 K, from dark to light, starting at the following values: (a) 294, (b) 291, (c) 288, and (d) 285 K.

For the DEEP-unif simulation, it is difficult to determine from system speed alone when the transition from density-current-like lifting to gravity-wave-like lifting occurs. However, cross sections reveal that the cold pool lifting gives way to the bore during the 5 h 30 min –7 h 30 min window (Fig. 16). Initially, the bore's speed is very close to that of the preexisting density current (as in section 3b). However, by $t = 7$ h 30 min the bore begins to outrun the density current; as the preoutflow stable layer becomes deeper and more stable, the bore's speed approaches that of a gravity wave, whose speed in turn continues to increase with increasing stability. In the "unif" simulations, the surface cold pool remains due to the uniform cooling technique; thus, the bore continually resembles the "lock release" (or intrusive density current) model. By roughly $t = 7$ h 30 min, this intrusive density current is subcritical, with internal gravity waves propagating ahead of it and an undular character to the bore (Fig. 16d).

In the case of the PJ04 environment, as reviewed previously, the transition to the elevated phase soon resulted in the demise of the system. In the DEEP environment, the system persisted as a weak, elevated,

fast-moving, bore-driven system through the remainder of the simulation. The overall interpretation is that, in order for the simulated convection to remain surface based, both CAPE and deep cold pool lifting need to persist. An important result is that this deep lifting may be best accomplished by somewhat weaker cold pools, which provide more upright trajectories for air parcels in the gust front updraft.

4. Synthesis

The present simulations are part of an ongoing effort to understand nocturnal convective systems, which are common in the United States. As a first attempt, artificial low-level cooling was added to simulations within environments that favor long-lived, quasi-steady convective systems. In the control simulations, these simulated convective systems are cold pool driven and surface based.

To varying degrees, the simulations that include continual low-level cooling evolve through four basic stages: strengthening, quasi steady, stalling, and elevated. During the strengthening stage, the surface cold pool develops and intensifies, the system speed increases, and the simulated convective systems become well organized. Then, during the quasi-steady stage, continued convective development along the system's outflow boundary leads to a surface-based squall line with nearly constant forward motion. During the quasi-steady stage, the outflow propagates and lifts environmental air as a density current. The strengthening and quasi-steady stages are common to all of the simulations, including the control runs.

Whereas the control and limited-cooling (e.g., 291 K) simulations remain within the quasi-steady stage, in the presence of continued cooling (the "unlim" experiment) the simulations progress into the stalling stage. As the low-level cooling renders a smaller cold pool temperature deficit (relative to the preline environment), a system's forward speed often decreases. Also, as the cold pool's strength (C) decreases in relation to the vertical wind shear (ΔU), a stalling system often exhibits a secondary peak in updraft strength and in the midlevel concentration of boundary layer tracers. This is consistent with the theory for strong gust front lifting developed by Rotunno et al. (1988). In simulations where the cold pool's temperature deficit is preserved during the cooling (the "unif" experiment), the stalling stage and its secondary maximum in system intensity are absent. Lifting during the stalling stage is by a bore in the stable layer, although the bore's speed and structure remain akin to those of a density current, and the bore's position is that of the original outflow's gust front.

For the simulations with unlimited cooling, the final stage is the transition to elevated convection. In this stage, surface parcels are no longer lifted to their LFC, either because of the extinction of CAPE (in the "unlim" experiments) or because of the lack of deep gust front lifting (in the "unif" experiments). As the low-level environment becomes increasingly stable, the outflow dynamics become akin to that of a gravity wave, and the system's speed increases. The near-surface flow branch is best described as "underflow"; despite some small vertical excursions in the vicinity of the bore, air in the stable layer mainly passes beneath the system without participating in the convection. In simulations with moist air above the stable layer (e.g., the DEEP experiments), the propagating bore is more than sufficient to lift elevated parcels to their LFC. In simulations with dry air above the stable layer (e.g., the PJ04 experiments), preline lifting and the release of potential instability also contribute, as the airmass aloft initially has low CAPE, high CIN, and requires significant lifting in order to achieve saturation and positive buoyancy.

There are no doubt many other pathways for elevated convective storms, especially those that occur above frontal inversions in the cold sectors of midlatitude cyclones (e.g., the "type 1" MCSs of Fritsch and Forbes 2001). The present results are somewhat novel in that no larger-scale front or low-level jet stream is required in order to sustain the simulated storms in an environment with a stable boundary layer. In the case where a surface-based squall line matures before it experiences low-level cooling, several key concepts emerge:

- A mechanism exists for the perpetuation of the squall line as the boundary layer stability increases. The evolution from a density current, to a density-current-like bore, and then to a gravity-wave-like bore provides continual lifting as the system becomes elevated. This evolution also entails changes in the squall line's forward speed.
- Some cooling of the preline environment can actually lead to an increase in the system's intensity, as the environmental shear can better offset the tendency for parcels to be swept rearward over the outflow.
- The lower troposphere can be cooled by a surprising amount (roughly 10 K) without disturbing the flow of surface-based parcels into a mature, cold-pool-driven squall line. Even when CAPE is small and CIN is large, the surface cold pool is sufficient to lift low-level parcels to their LFC.

The present simulations are meant to mimic the impacts of nocturnal cooling upon existing squall lines.

The implications are that active convective systems can survive after sunset, and can even intensify. Furthermore, many of the nocturnal convective systems that were previously thought to be elevated may actually be surface based.

5. Future avenues

This study isolated one particular aspect of a nocturnal-like evolution in the convective environment. However, over the central United States, low-level jets also frequently develop at night. Future studies might consider the role of the changing wind profile (and, thus, changing vertical wind shear) in addition to the role of low-level cooling. Another interesting question is whether supercellular thunderstorms are more or less able to survive and remain surface based into the nighttime hours. Although they do not generally possess strong, deep mesoscale cold pools, supercells often produce minimized pressure aloft (e.g., Klemp 1987), which can contribute to the dynamic lifting of air that has appreciable CIN. Whether or not supercells can remain surface based in the presence of low-level cooling has profound impacts for the tornado forecast problem.

Although this paper's primary emphasis is not the production of severe winds, it is worthwhile to note that severe surface wind production ceased around the same time that the simulated systems became elevated. The problem of severe convective winds in stable environments continues to be a challenge. Even in the absence of surface-based CAPE, elevated convective systems may produce negatively buoyant downdrafts that are strong enough to penetrate to the surface. Alternatively, as suggested by Schmidt and Cotton (1989) and Bernardet and Cotton (1998), stable surface air that is present near an elevated convective system can be dynamically lifted and cooled at the system's gust front, after which it returns rapidly to the surface owing to its negative buoyancy. Finally, a mature elevated system might produce a sufficiently perturbed pressure field (e.g., Fig. 9) such that the subinversion air, even if decoupled from the convective overturning, can yet be accelerated to severe speed. Recent preliminary work by Bryan and Weisman (2006) has also shown that initially elevated squall lines can produce cold pools that build downward to the surface over time, eventually producing severe surface winds in much the same way that surface-based systems do. Still other preliminary results from Atkins and Cunningham (2006) have shown that stable layers can inhibit formation of the embedded low-level mesovortices that may often be the direct cause of a squall line's severe surface winds (e.g., Trapp and Weisman 2003; Atkins et al. 2005). Going forward, it is important to understand these severe wind mechanisms, and to assess the generality of the current and previous findings.

In the central United States, a large fraction of convective storms occur at night. Future advances in our understanding of the dynamics that govern nocturnal storms, and their likelihood of producing severe weather, will be important additions to the knowledge base.

Acknowledgments. The author would like to thank N. Atkins, G. Bryan, R. Fovell, P. Haertel, R. Johnson, K. Knupp, E. Kuchera, P. Markowski, and the Convective Storms Group at NC State for beneficial discussions and suggestions related to this work. Both R. Fovell and M. Weisman provided constructive reviews of the original manuscript. G. Bryan also kindly assisted by providing and supporting the numerical model used for this work. This research was supported by the National Science Foundation under Grant ATM-0552154.

REFERENCES

Atkins, N. T., and J. J. Cunningham, 2006: The influence of low-level stable layers on damaging surface winds within bow echoes. Preprints, *23rd Conf. on Severe Local Storms,* St. Louis, MO, Amer. Meteor. Soc., 6.4.

——, C. S. Bouchard, R. W. Przybylinski, R. J. Trapp, and G. Schmocker, 2005: Damaging surface wind mechanisms within the 10 June 2003 Saint Louis bow echo during BAMEX. *Mon. Wea. Rev.,* **133,** 2275–2296.

Bernardet, L. R., and W. R. Cotton, 1998: Multiscale evolution of a derecho-producing mesoscale convective system. *Mon. Wea. Rev.,* **126,** 2991–3015.

Braun, S. A., and W.-K. Tao, 2000: Sensitivity of high-resolution simulations of Hurricane Bob (1991) to planetary boundary layer parameterizations. *Mon. Wea. Rev.,* **128,** 3941–3961.

Bryan, G. H., and J. M. Fritsch, 2002: A benchmark simulation for moist nonhydrostatic numerical models. *Mon. Wea. Rev.,* **130,** 2917–2928.

——, and M. L. Weisman, 2006: Mechanisms for the production of severe surface winds in a simulation of an elevated convective system. Preprints, *23rd Conf. on Severe Local Storms,* St. Louis, MO, Amer. Meteor. Soc., 7.5.

——, and R. Rotunno, 2008: Gravity currents in a deep anelastic atmosphere. *J. Atmos. Sci.,* **65,** 536–556.

——, J. C. Wyngaard, and J. M. Fritsch, 2003: Resolution requirements for the simulation of deep moist convection. *Mon. Wea. Rev.,* **131,** 2394–2416.

——, J. C. Knievel, and M. D. Parker, 2006: A multimodel assessment of RKW theory's relevance to squall-line characteristics. *Mon. Wea. Rev.,* **134,** 2772–2792.

Buzzi, A., M. Fantini, and G. Lippolis, 1991: Quasi-stationary organized convection in the presence of an inversion near the surface: Experiments with a 2-D numerical model. *Meteor. Atmos. Phys.,* **45,** 75–86.

Carbone, R. E., J. W. Conway, N. A. Crook, and M. W. Moncrieff, 1990: The generation and propagation of a nocturnal

squall line. Part I: Observations and implications for mesoscale predictability. *Mon. Wea. Rev.,* **118,** 26–49.

Colman, B. R., 1990: Thunderstorms above frontal surfaces in environments without positive CAPE. Part I: A climatology. *Mon. Wea. Rev.,* **118,** 1103–1121.

Coniglio, M. C., and D. J. Stensrud, 2001: Simulation of a progressive derecho using composite initial conditions. *Mon. Wea. Rev.,* **129,** 1593–1616.

Cotton, W. R., R. L. George, P. J. Wetzel, and R. L. McAnelly, 1983: A long-lived mesoscale convective complex. Part I: The mountain-generated component. *Mon. Wea. Rev.,* **111,** 1893–1918.

Dudhia, J., M. W. Moncrieff, and D. W. K. So, 1987: The two-dimensional dynamics of West African squall lines. *Quart. J. Roy. Meteor. Soc.,* **113,** 121–146.

Fovell, R. G., 2002: Upstream influence of numerically simulated squall-line storms. *Quart. J. Roy. Meteor. Soc.,* **128,** 893–912.

——, G. L. Mullendore, and S.-H. Kim, 2006: Discrete propagation in numerically simulated nocturnal squall lines. *Mon. Wea. Rev.,* **134,** 3735–3752.

Fritsch, J. M., and G. S. Forbes, 2001: Mesoscale convective systems. *Severe Convective Storms, Meteor. Monogr.,* No. 50, Amer. Meteor. Soc., 323–357.

Glickman, T. S., Ed., 2000: *Glossary of Meteorology.* 2nd ed. American Meteorological Society, 855 pp.

Haertel, P. T., R. H. Johnson, and S. N. Tulich, 2001: Some simple simulations of thunderstorm outflows. *J. Atmos. Sci.,* **58,** 504–516.

Holton, J. R., 2004: *An Introduction to Dynamic Meteorology.* 4th ed. International Geophysical Series, Vol. 88, Academic Press, 535 pp.

Johns, R. H., and W. D. Hirt, 1987: Derechos: Widespread convectively induced windstorms. *Wea. Forecasting,* **2,** 32–49.

Klemp, J. B., 1987: Dynamics of tornadic thunderstorms. *Annu. Rev. Fluid Mech.,* **19,** 369–402.

——, R. Rotunno, and W. C. Skamarock, 1997: On the propagation of internal bores. *J. Fluid Mech.,* **331,** 81–106.

Knupp, K. R., 2006: Observational analysis of a gust front to bore to solitary wave transition within an evolving nocturnal boundary layer. *J. Atmos. Sci.,* **63,** 2016–2035.

Kuchera, E. L., and M. D. Parker, 2006: Severe convective wind environments. *Wea. Forecasting,* **21,** 595–612.

Lin, Y.-L., R. D. Farley, and H. D. Orville, 1983: Bulk parameterization of the snow field in a cloud model. *J. Climate Appl. Meteor.,* **22,** 1065–1092.

Liu, C., and M. W. Moncrieff, 2000: Simulated density currents in idealized stratified environments. *Mon. Wea. Rev.,* **128,** 1420–1437.

Locatelli, J. D., M. T. Stoelinga, P. V. Hobbs, and J. Johnson, 1998: Structure and evolution of an undular bore on the high plains and its effect on migrating birds. *Bull. Amer. Meteor. Soc.,* **79,** 1043–1060.

Maddox, R. A., 1980: Mesoscale convective complexes. *Bull. Amer. Meteor. Soc.,* **61,** 1374–1387.

——, 1983: Large-scale meteorological conditions associated with midlatitude mesoscale convective complexes. *Mon. Wea. Rev.,* **111,** 1475–1493.

Mapes, B. E., 1993: Gregarious tropical convection. *J. Atmos. Sci.,* **50,** 2026–2037.

Nicholls, M. E., R. A. Pielke, and W. R. Cotton, 1991: Thermally forced gravity waves in an atmosphere at rest. *J. Atmos. Sci.,* **48,** 1869–1884.

Parker, M. D., and R. H. Johnson, 2004: Structures and dynamics of quasi-2D mesoscale convective systems. *J. Atmos. Sci.,* **61,** 545–567.

Raymond, D. J., and R. Rotunno, 1989: Response of a stably stratified flow to cooling. *J. Atmos. Sci.,* **46,** 2830–2837.

Rottman, J. W., and J. E. Simpson, 1989: The formation of internal bores in the atmosphere: A laboratory model. *Quart. J. Roy. Meteor. Soc.,* **115,** 941–963.

Rotunno, R., J. B. Klemp, and M. L. Weisman, 1988: A theory for strong, long-lived squall lines. *J. Atmos. Sci.,* **45,** 463–485.

Schmidt, J. M., and W. R. Cotton, 1989: A high plains squall line associated with severe surface winds. *J. Atmos. Sci.,* **46,** 281–302.

——, and W. R. Cotton, 1990: Interactions between upper and lower tropospheric gravity waves on squall line structure and maintenance. *J. Atmos. Sci.,* **47,** 1205–1222.

Stensrud, D. J., M. C. Coniglio, R. P. Davies-Jones, and J. S. Evans, 2005: Comments on "'A theory for strong long-lived squall lines' revisited." *J. Atmos. Sci.,* **62,** 2989–2996.

Trapp, R. J., and M. L. Weisman, 2003: Low-level mesovortices within squall lines and bow echoes. Part II: Their genesis and implications. *Mon. Wea. Rev.,* **131,** 2804–2823.

Trier, S. B., and D. B. Parsons, 1993: Evolution of environmental conditions preceding the development of a nocturnal mesoscale convective complex. *Mon. Wea. Rev.,* **121,** 1078–1098.

——, C. A. Davis, D. A. Ahijevych, M. L. Weisman, and G. H. Bryan, 2006: Mechanisms supporting long-lived episodes of propagating nocturnal convection within a 7-day WRF model simulation. *J. Atmos. Sci.,* **63,** 2437–2461.

Wallace, J. M., 1975: Diurnal variations in precipitation and thunderstorm frequency over the conterminous United States. *Mon. Wea. Rev.,* **103,** 406–419.

Weisman, M. L., and J. B. Klemp, 1982: The dependence of numerically simulated convective storms on vertical wind shear and buoyancy. *Mon. Wea. Rev.,* **110,** 504–520.

——, and R. Rotunno, 2004: "A theory for strong long-lived squall lines" revisited. *J. Atmos. Sci.,* **61,** 361–382.

Wetzel, P. J., W. R. Cotton, and R. L. McAnelly, 1983: A long-lived mesoscale convective complex. Part II: Evolution and structure of the mature complex. *Mon. Wea. Rev.,* **111,** 1919–1937.